Optical Materials 35 (2013) 563–566

Contents lists available at SciVerse ScienceDirect

Optical Materials

journal homepage: www.elsevier.com/locate/optmat

Optical properties of polyvinyl alcohol (PVA) coated In_2O_3 nanoparticles

Dali Shao *, Liqiao Qin, Shayla Sawyer

Electrical, Computer, and Systems Engineering Department, Rensselaer Polytechnic Institute, Troy, NY 12180, USA

ARTICLE INFO

Article history:
Received 28 February 2012
Received in revised form 25 September 2012
Accepted 12 October 2012
Available online 27 November 2012

Keywords:
Indium oxide (In_2O_3) nanoparticles
Polyvinyl-alcohol (PVA)
UV photodetector
Surface passivation

ABSTRACT

An experimental study of the optical properties of PVA coated In_2O_3 nanoparticles was performed with characterization methods including photoluminescence, absorption and point source, photogenerated current–voltage measurements. The photoluminescence results show that PVA can suppress the parasitic green emission by modifying defect energy states introduced by oxygen vacancies. Thin films fabricated from PVA coated In_2O_3 nanoparticles show higher photocurrent and suppressed dark current, which may be promising for UV photodetector applications.

1. Introduction

Low-dimensional, metal oxide semiconductor nanomaterials have stimulated great interest and extensive research due to their novel electronic and optical properties. Among them, In_2O_3 is a wide band-gap semiconductor material that has a variety of applications including: field effect transistors (FETs) [1–3], gas sensing [4–6] and optoelectronic devices [7–9]. However, one prominent issue for In_2O_3 nanomaterials is the parasitic blue–green emission, due to oxygen vacancies [10–14]. This parasitic emission was also observed in ZnO nanostructures [15–20]. Research has begun to investigate the effective use of surface modification [21–23] to solve this problem for ZnO nanoparticles. To our knowledge, methods to suppress parasitic green emission for In_2O_3 nanoparticles have not been studied yet.

In this paper, the material characteristics of a thin film fabricated from polyvinyl-alcohol (PVA) coated In_2O_3 nanoparticles are investigated. Compared to uncoated In_2O_3 nanoparticles, significant suppression of the parasitic green emission and enhanced UV–blue emission is demonstrated, proving that PVA can modify defect levels in this material.

2. Experiment

The thin films were fabricated from commercial In_2O_3 nanoparticles (US Research Nanomaterials Inc.) with a purity of 99.995% and sizes ranging from 20 to 70 nm. They were divided into two batches. The first batch was dispersed in ethanol to form 40 mg/ml suspension. The second batch was treated with PVA solutions (1% in weight in water), providing surface passivation. Then the PVA coated In_2O_3 nanoparticles were centrifuged and dispersed in ethanol. The concentration of the suspension was also 40 mg/ml. These solutions were then spin-coated onto quartz plates and annealed in air at 120 °C for 5 min, respectively.

The following characterization methods were used to determine the material quality and optical characteristics of the In_2O_3 nanoparticles. A Carl Zeiss Ultra 1540 dual beam scanning electron microscope (SEM) was used to determine size and morphology. Photoluminescence (PL) spectra were measured using a Spex Fluorolog Tau-3 spectrofluorimeter with a Xenon lamp and the excitation wavelength was fixed at 330 nm. UV–Vis absorption spectra were recorded using a Shimadzu UV–Vis 2550 spectrophotometer with a deuterium lamp (190–390 nm) and a halogen lamp (280–1100 nm). Auto switching between the lamps is synchronized to a wavelength and the switching range is selectable between 282 and 393 nm. The scanning wavelength range used in the experiment is 240–800 nm with a switching wavelength of 330 nm. Dark current and photogenerated current were measured using a HP4155B semiconductor parameter analyzer and a UV LED with peak wavelength at 335 nm. All measurements were performed at room temperature in air.

3. Results and discussion

Fig. 1 is a high resolution SEM image of PVA coated In_2O_3 nanoparticles spin-coated onto a quartz substrate. The sizes of the nanoparticles are in the range of 20–70 nm with an average value of approximately 40 nm. The uncoated In_2O_3 nanoparticles in ethanol spin-coated onto quartz substrate exhibit a similar size.

* Corresponding author.
E-mail address: shaodali828@gmail.com (D. Shao).

0925-3467/$ - see front matter © 2012 Elsevier B.V. All rights reserved.
http://dx.doi.org/10.1016/j.optmat.2012.10.026

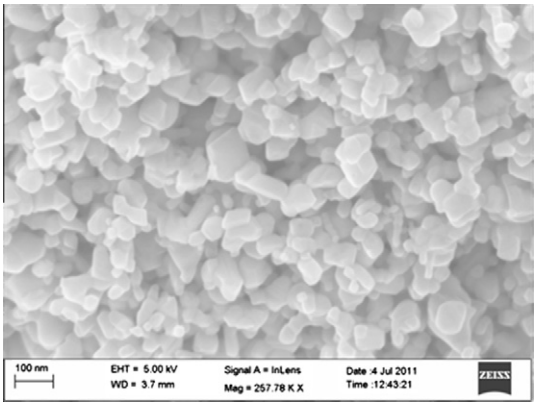

Fig. 1. High resolution SEM image of PVA coated In_2O_3 nanoparticles.

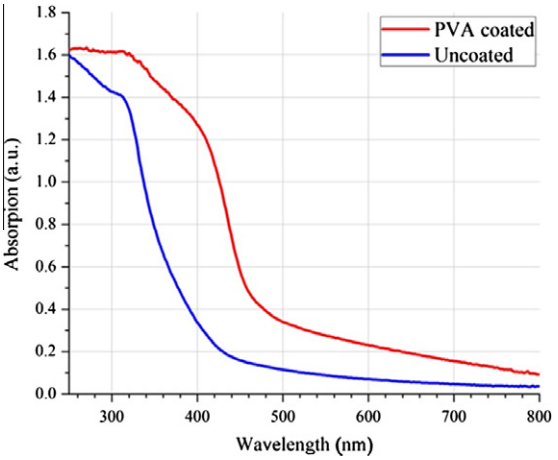

Fig. 3. Absorption spectra demonstrate higher UV and blue absorption for PVA coated In_2O_3 nanoparticles comparing with uncoated In_2O_3 nanoparticles.

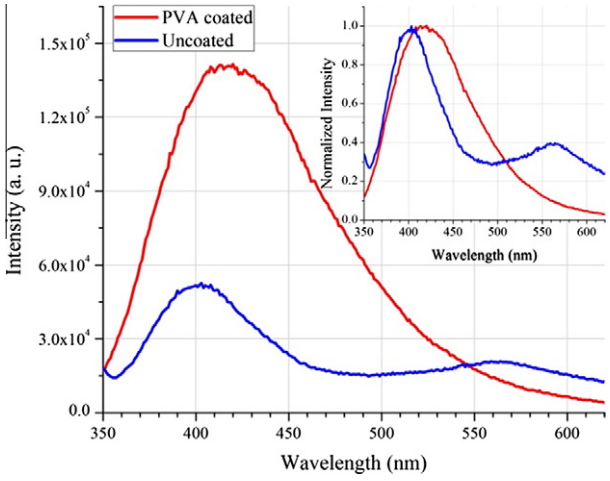

Fig. 2. PL spectra of In_2O_3 excited at 335 nm show enhanced UV–blue emission and suppressed green emission by PVA coating. (The inset is the normalized spectra.)

The PL spectra of PVA coated and uncoated In_2O_3 nanoparticles are presented in Fig. 2 Two broad bands are observed from the uncoated sample. The first band with peak at 402 nm (3.08 eV) is close to the newly revised fundamental band-gap of In_2O_3 (2.93 ± 0.15 eV) by recent studies [24–26]. Theoretical calculations from these studies have shown that transitions from the first six valence bands into the conduction band are either symmetry forbidden or have very low dipole intensity. A review of available literature on the emission spectra of nanostructured In_2O_3 show that the emission spectra of nanostructured In_2O_3 strongly depend on morphology and growth conditions of the nanostructures .The emission peak at 3.08 eV is very close to the UV emission peak (3.18 eV) observed for ZnO nanowires by Gali et al. [27]. Guha et al. and Liang et al. reported PL emission at 2.64 eV from In_2O_3 nanopyramids and nanocolumns and a broad emission peak at the same energy for nano-fiblers respectively [13,28]. Whereas, Jean et al. reported PL emission peak at 2.13 eV from In_2O_3 nanotowers [29]. Therefore, a range of PL emissions are found in literature due to the many possible transitions around the band-gap.

The second band is parasitic green emission with a peak at 565 nm. When excited at 335 nm, the PL spectra clearly indicate that the PVA coating enhanced UV–blue emission and diminished parasitic green emission. In addition, the PL peak shifted from 402 nm to 420 nm and the full width at half maximum (FWHM) expands from 74 nm to 110 nm. The shift of the PL spectra is likely due to the defect-related transitions rather than the quantum confinement effect. The diameter of the In_2O_3 nanoparticles in this study is much larger than the critical Bohr radius of In_2O_3 (2.38 nm) [30]; therefore, the quantum confinement effect can be excluded. The origin of photoluminescence in In_2O_3 was attributed to amorphous indium oxide or oxygen vacancies [31]. However, recent studies show other defects like oxygen antisites, indium interstitials, oxygen interstitials, and indium vacancies were also found to be responsible for PL emission in In_2O_3 [32,33]. In general, the various effects listed above provide additional transition paths for carriers through energy states created by the defects [34,35]. Several recent studies show that polymers such as polymethyl methacrylate (PMMA) and PVA can effectively modify surface defect states of metal oxide by covering the surface of metal oxide through a large amount of hydroxyl groups [36–38]. Thus, the shift and expansion of the PL spectra in this work may be explained as a modification of surface defect states due to the PVA coating, leading to additional carrier transition paths. This conclusion is further supported by the absorption spectra presented in Fig. 3, which show enhanced UV–blue absorption due to surface defect level modification.

The parasitic green emission observed in uncoated In_2O_3 nanoparticles is attributed to the oxygen vacancies that induce deep donor defect levels within the band-gap of In_2O_3 nanostructures [10–14]. A similar defect level emission (DLE) mechanism is found in other metal oxides including ZnO [15–20]. Based on explanation given by van Dijken et al. [39] and a model proposed by Jan-Peter Richters et al. [36] that illustrate the influence of polymer coating on ZnO nanowires, here we developed a model that explain the decreased intensity of the DLE for PVA coated In_2O_3 nanoparticles and this model is shown in Fig. 4. According to van Dijken et al., the DLE cannot be generated from recombination of electrons with single charged oxygen vacancies centers (V_o^+), but generated by recombination between electrons and double charged oxygen vacancies centers (V_o^{2+}). These V_o^{2+} centers are formed through two mainly steps. First, the photogenerated holes are trapped by surface adsorbed oxygen ions (O^- and O_2^-) through a very fast process. Second, the holes may tunnel into the deep-level defects to create the optically active V_o^{2+} centers. Due to the large surface to volume ratio of In_2O_3 nanoparticles, the two step process can be very strong, which introduce considerable amount of V_o^{2+} centers and therefore DLE. Due to the changed dielectric constant of the surrounding material introduced by PVA coating, the local electric structures of In_2O_3 nanoparticles are changed. This can effectively reduce the density of the surface adsorbed O^- and O_2^- due to screening effect [36]. Therefore, fewer holes will be trapped

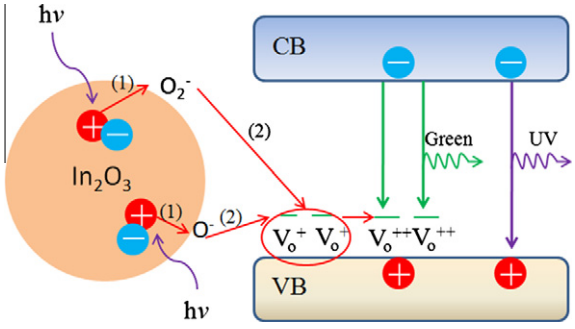

Fig. 4. Schematic diagram illustrating the mechanism of DLE in In_2O_3 nanoparticles.

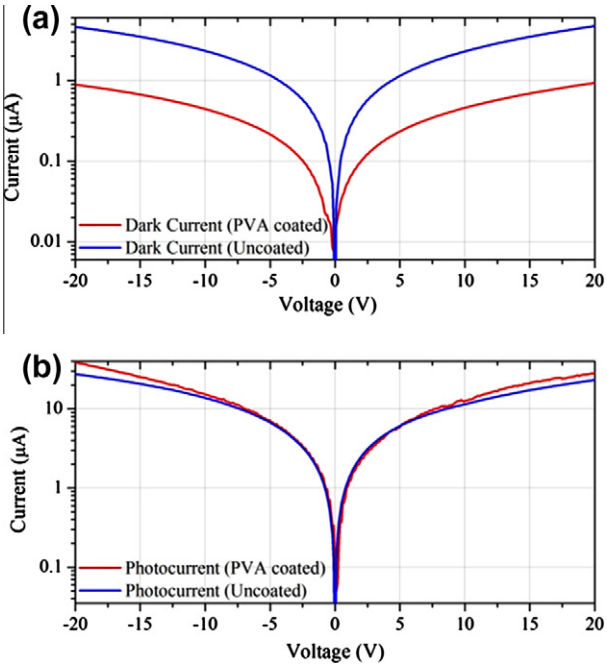

Fig. 5. (a) Dark current and (b) photocurrent measured from PVA coated and uncoated photodetectors.

at the surface of In_2O_3, leading to reduced density of V_o^{2+} centers and hence reduced DLE.

The current–voltage (I–V) characteristics for thin films fabricated from PVA coated and uncoated In_2O_3 nanoparticles, shown in Fig. 5, were measured by two tungsten needles touching the film surface directly. The measurements were done under dark and illumination using a 335 nm UV LED with intensity of 31.65 mW/cm^2. The photocurrent measured from the PVA coated sample is slightly higher than the uncoated sample, while the dark current of PVA coated sample is only one fifth of uncoated sample. Due to the reduced density of surface defects by PVA passivation, the suppressed dark current is expected. For the photocurrent of the In_2O_3 nanoparticles, the oxygen vacancy defects and surface adsorbed oxygen molecules are two important factors need to be discussed. First, the oxygen vacancy defects usually act as carrier trapping centers and can reduce the photocurrent by trapping the photo-generated carriers before they reach the contacts. Thus a decrease in the density of surface oxygen vacancy sites also leads to a reduced number of carrier trapping centers, which enhances the photocurrent collection efficiency. Second, PVA passivation reduces the surface adsorbed oxygen molecules and increases the free carrier concentration inside the In_2O_3 nanoparticles film. This mechanism is similar as the interaction between In_2O_3 and Ozone [40–42]. Several recent studies demonstrated that In_2O_3 films as well as nanoparticles have a high accumulation of surface electrons [24,43,44]. Oxygen molecules are adsorbed onto In_2O_3 surface to form negative charged oxygen ions (O^-, O_2^- and O_3^-) and capture free electrons from the In_2O_3, leading a decrease of free carrier concentration inside of the In_2O_3 nanoparticles [40,42]. This oxygen adsorption usually occurs on the surface oxygen vacancy sites, which often dominate the electronic/chemical properties and adsorption behaviors of metal oxide surfaces [45,46]. Upon the UV illumination, the surface adsorbed oxygen from a bound to the gaseous state. In the resulting vacancies, the two electrons of the oxygen ion are left in the vacant site and can contribute to the density of free carriers [41]. Due to the surface passivation of In_2O_3 by PVA, the density of surface oxygen vacancies are reduced and so are the surface adsorbed oxygen molecules. This can increase the free carrier concentration inside the In_2O_3 and enhance the photocurrent. Moreover, the thin film fabricated from PVA coated In_2O_3 nanoparticles can be modeled as a disordered hopping system, in which the effective mobility of carriers is strongly dependent on free carrier concentrations [31,47]. The effects above will further enhance the photocurrent of the device.

4. Conclusion

In conclusion, enhanced UV–blue emission and suppressed parasitic green emission has been observed in PVA coated In_2O_3 nanoparticles. Thin film based on this material shows higher photocurrent sensitivity. These results indicate that PVA can be used to passivate In_2O_3 nanoparticles and enhance the performance of photodetector in the UV–blue region created from this material.

Acknowledgements

The authors gratefully acknowledge support from National Security Technologies through NSF Industry/University Cooperative Research Center Connection One. The authors also acknowledge the National Science Foundation Smart Lighting Engineering Research Center (EEC-0812056).

References

[1] C. Li, D.H. Zhang, X.L. Liu, S. Han, T. Tang, J. Han, C.W. Zhou, Appl. Phys. Lett. 82 (2003) 1613.
[2] J. Kong, N.R. Franklin, C.W. Zhou, M.G. Chapline, S. Peng, K.J. Cho, H.J. Dai, Science 287 (2000) 622.
[3] A. Kolmakov, M. Moskovits, Ann. Rev. Mater. Res. 34 (2004) 151.
[4] G. Korotcenkov, A. Cerneavschi, V. Brinzari, A. Vasiliev, M. Ivanov, A. Cornet, J. Morante, A. Cabot, J. Arbiol, Sens. Actuators B – Chem. 99 (2004) 297.
[5] M. Ivanovskaya, A. Gurlo, P. Bogdanov, Sens. Actuators B – Chem. 77 (2001) 264.
[6] G. Neri, A. Bonavita, G. Micali, G. Rizzo, N. Pinna, M. Niederberger, Sens. Actuators B – Chem. 127 (2007) 455.
[7] L.C. Chen, Phys. J. Appl. Phys. 35 (2006) 13–15.
[8] K.L. Chopra, S. Major, D.K. Pandya, Thin Solid Films 102 (1983) 1.
[9] D.S. Ginley, C. Bright, Mater. Res. Soc. Bull. 25 (2000) 15.
[10] X.P. Shen, H.J. Liu, X. Fan, Y. Yuan, J.M. Hong, Z. Xu, J. Cryst. Growth 276 (2005) 471.
[11] L. Dai, X.L. Chen, J.K. Jian, M. He, T. Zhou, B.Q. Hu, Appl. Phys. A 75 (2002) 687.
[12] M.J. Zheng, L.D. Zhang, G.H. Li, X.Y. Zhang, X.F. Wang, Appl. Phys. Lett. 79 (2001) 839.
[13] P. Guha, S. Kar, S. Chaudhuri, Appl. Phys. Lett. 85 (2004) 3851.
[14] Q. Tang, W. Zhou, W. Zhang, S. Ou, K. Jiang, W. Yu, Y. Qian, Cryst. Growth Des. 5 (2005) 147–150.
[15] L. Qin, C. Shing, S. Sawyer, P.S. Dutta, Opt. Mater. 33 (2011) 359–362.
[16] S. Monticone, R. Tufeu, A. Kanaev, J. Phys. Chem. B 102 (1998) 2854.
[17] Y. Wu, A. Tok, F. Boey, X. Zeng, X. Zhang, Appl. Surf. Sci. 253 (2007) 5473.
[18] L. Wu, Y. Wu, X. Pan, F. Kong, Opt. Mater. 28 (2006) 418.
[19] V.A. Fonoberov, A.A. Balandin, Appl. Phys. Lett. 85 (2004) 597.
[20] V.A. Fonoberov, K.A. Alim, A.A. Balandin, Phys. Rev. B. 73 (2006) 165317.
[21] H. Xiong, Z. Wang, Y. Xia, Adv. Mater. 18 (2006) 748.

[22] L. Guo, S. Yang, C. Yang, P. Yu, J. Wang, W. Ge, G. Wong, Appl. Phys. Lett. 76 (2000) 2901.
[23] S. Mridha, M. Nandi, A. Bhaumik, D. Basak, Nanotechnology 19 (2008) 275705.
[24] P.D.C. King, T.D. Veal, F. Fuchs, Ch.Y. Wang, D.J. Payne, A. Bourlange, H. Zhang, G.R. Bell, V. Cimalla, O. Ambacher, R.G. Egdell, F. Bechstedt, C.F. McConville, Phys. Rev. B 79 (2009) 205211.
[25] A. Walsh, J.L.F. Da Silva, S.-H. Wei, C. Korber, A. Klein, L.F.J. Piper, A. DeMasi, K.E. Smith, G. Panaccione, P. Torelli, D.J. Payne, A. Bourlange, R.G. Egdell, Phys. Rev. Lett. 100 (2008) 167402.
[26] L.F.J. Piper, A. DeMasi, S.W. Cho, K.E. Smith, F. Fuchs, F. Bechstedt, C. Körber, A. Klein, D.J. Payne, R.G. Egdell, Appl. Phys. Lett. 94 (2009) 022105.
[27] P. Gali, F.-L. Kuo, N. Shepherd, U. Philipose, Semicond. Sci. Technol. 27 (2012) 015015.
[28] C.H. Liang, G.W. Meng, Y. Lei, F. Phillipp, L.D. Zhang, Adv. Mater. 13 (2001) 1330.
[29] S.-T. Jean, Y.-C. Her, Cryst. Growth Des. 10 (2010) 5.
[30] F. Zeng, X. Zhang, J. Wang, L. Wang, L. Zhang, Nanotechnology 15 (2004) 596–600.
[31] V.I. Arkhipov, P. Heremans, E.V. Emelianova, G.J. Adriaenssens, H. Bassler, Appl. Phys. Lett. 82 (2003) 3245–3247.
[32] E.C.C. Souza, J.F.Q. Rey, E.N.S. Muccillo, Appl. Surf. Sci. 255 (2009) 3779–3783.
[33] M. Kumar, V.N. Singh, F. Singh, K.V. Lakshmi, B.R. Mehta, J.P. Singh, Appl. Phys. Lett. 92 (2008) 171907.
[34] T.-S. Ko, C.-P. Chu, J.-R. Chen, T.-C. Lu, H.-C. Kuo, S.-C. Wang, J. Cryst. Growth 310 (2008) 2264.
[35] K.B. Sundaram, G.K. Bhagavat, Phys. Status Sol. 63 (1983) K15.
[36] J.-P. Richters, T. Voss, L. Wischmeier, I. Rückmann, J. Gutowski, Appl. Phys. Lett. 92 (2008) 011103.
[37] T.K. Kundu, N. Karak, P. Barik, S. Saha, Int. J. Soft Comput. Eng. 1 (2011) 19.
[38] K.W. Liu, R. Chen, G.Z. Xing, T. Wu, H.D. Sun, Appl. Phys. Lett. 96 (2010) 023111.
[39] A. van Dijken, E.A. Meulenkamp, D. Vanmaekelbergh, A. Meijerink, J. Phys. Chem. B 104 (2000) 1715–1723.
[40] A. Gurlo, N. Barsan, U. Weimar, M. Ivanovskaya, A. Taurino, P. Siciliano, Chem. Mater. 15 (2003) 4377–4383.
[41] G. Kiriakidis, M. Bender, N. Katsarakis, E. Gagaoudakis, E. Hourdakis, E. Douloufakis, V. Cimalla, Phys. Stat. Sol. (a) 185 (2001) 27–32.
[42] V. Golovanov, Matti A. Maki-Jaskari, Tapio T. Rantala, G. Korotcenkov, V. Brinzari, A. Cornet, J. Morante, Sens. Actuators B – Chem. 106 (2005) 563–571.
[43] P.D.C. King, T.D. Veal, D.J. Payne, A. Bourlange, R.G. Egdell, C.F. McConville, Phys. Rev. Lett. 101 (2008) 116808.
[44] M. Himmerlich, Ch.Y. Wang, V. Cimalla, O. Ambacher, S. Krischok, J. Appl. Phys. 111 (2012) 093704.
[45] V.E. Henrich, P.A. Cox, The Surface Science and Metal Oxides, Cambridge University Press, Cambridge, 1994.
[46] R. Schaub, E. Wahlstrom, A. Ronnaus, E. Laegsgaard, I. Stensgaard, F. Besenbacher, Science 299 (2003) 377–379.
[47] E.V. Emelianova, M. van der Auweraer, G.J. Adriaenssensand, A. Stesmans, Org. Electron. 9 (2008) 129–135.